Structural and kinematic analysis of the Early Paleozoic Ondor Sum-Hongqi mélange belt, eastern part of the Altaids (CAOB) in Inner Mongolia, China

Guanzhong Shi, Michel Faure, Bei Xu, Pan Zhao, Yan Chen

Structural and kinematic analysis of the Early Paleozoic Ondor Sum-Hongqi mélange belt, eastern part of the Altaids (CAOB) in Inner Mongolia, China

Guanzhong Shi [a,b] Michel Faure[b], Bei Xu[a,*], Pan Zhao[a,b], Yan Chen[b]

[a] Key Laboratory of Orogenic Belts and Crustal Evolution, Ministry of Education, Peking University, Beijing, 100871, China

[b] Institut des Sciences de la Terre d'Orléans, UMR Université d'Orléans-INSU/CNRS 7327, 1A rue de la Férollerie, 45071 Orléans, Cedex 2, France

[*]Corresponding author E-mail address: bxu@pku.edu.cn

Abstract

We present a stuctural and kinematic study of an Early Paleozoic subduction mélange and a magmatic arc that form the main elements of the Southern Orogen Belt of Inner Mongolia, which lies in the eastearn part of the Altaids or Central Asia Orogenic Belt. The structural analysis of the mélange conducted in the Hongqi and Ondor Sum areas (western Inner Mongolia) shows two phrases of ductile deformation. The D_1 event is responsible for the pervasive S_1 foliation, NW-SE striking L_1 stretching lineation and F_1 intrafolial folds. These microstructures are coeval with a greenschist facies metamorphism. During D_2, NW-verging F_2 folds associated with a S_2 axial planar cleavage deformed S_1 and L_1. The D_1 kinematic criteria indicate a top-to-the-NW sense of shear. D_1 and D_2 developed before the unconformable deposition of the Early Devonian shallow water sandstone. A lithosphere scale geodynamic model involving

an Early Paleozoic southeast-directed subduction beneath the North China Craton and late Silurian collision of the North China Craton with an hypothetical microcontinent is proposed to account for the microstructural evolution.

Key words: Accretionary orogen; Altaids (CAOB); Inner Mongolia; Early Paleozoic collision.

1. Introduction

Accretionary orogens, formed at active plate margins, play a major role in continental growth either vertically by transfer of mantle material within the crust in magmatic arcs or horizontally by accretion of oceanic material (i.e. magmatic island arcs, sea-mounts, oceanic crust and its sedimentary cover) against the continental margin (e.g. Condie et al., 2007; Cawood et al., 2009). Accretionary orogens are widespread in Central and East Asia. The Paleozoic accretionary orogens, recognized from the Urals Mts to Inner Mongolia in NE China, are called Altaids (Altaid Tectonic Collage, Sengor et al., 1993; Sengor and Natal'in, 1996) or Central Asia Orogenic Belt (CAOB, Jahn, 2004; Xiao et al., 2003, 2008; Windley et al., 2007). The Altaids/CAOB represents the consumption and remnant of the Paleo-Asian Ocean, currently preserved as ophiolite and serpentinite mélanges. This belt occupies an area of more than 5000 km long and 300 km wide. The end of the oceanic subduction and accretionary process is a critical point in the evolution of any accretionary orogen. Several possibilities have been suggested. Strike-slip tectonics along plate margins may lead to oblique

subduction and collage (e.g. Sengor et al., 1993; Choulet et al., 2012). Another possibility is that the stopping of oceanic subduction is due to the entrance of a buoyant feature such as a magmatic arc or a microcontinent in the subduction channel (Condie et al., 2007; Cawood et al., 2009).

The eastern segment of the Altaids/CAOB is mainly exposed in Inner Mongolia. The Solonker (also called Solon Obo) suture is considered as the major structure that delineates the location of the Paleo-Asian Ocean (Xiao et al., 2003; Windly et al., 2007; Chen et al., 2009; Jian et al., 2010). Xiao et al (2003) considered that during the Late Precambrian to Cambrian a north-directed subduction gave rise to the Ulan arc, and during the Early Paleozoic, a south-directed oceanic subduction below the North China Craton was coeval with a north-directed oceanic subduction below the southern Mongolian margin. Finally, in Late Permian to Early Triassic, the two opposite subduction systems came into contact to give rise to the Solonker suture. However, the Paleozoic tectonic evolution of this area is also interpreted as the result of two opposite subductions and collisions during the Middle Paleozoic (Xu and Chen, 1993; 1997; Xu et al., 2012).

The Southern Orogenic Belt (SOB) is equivalent to the Manchurides (Hsu et al. 1991; Sengor and Natal'in, 1996). Xu et al., (2012) argued that during the Early Paleozoic, a south-directed oceanic subduction took place below the North China Craton, and that the subduction system ended around 420-380Ma. Recently, paired metamorphic belts were reported in the Bainaimiao and the Ondor Sum areas, and the age of 411 ± 8Ma for undeformed pegmatite dike was regarded as upper limit of the

collision (Zhang et al., 2012). Despite the existence of several geodynamic scenarios, the structural and kinematic features of the south-directed subduction are poorly constrained. This paper deals with the western part of the Southern Orogenic Belt that extends from Hongqi to Ondor Sum, in the west, and east, respectively (Fig. 1). In the following, two main questions will be addressed, namely: i) what is the bulk geometry and kinematics deduced from microtectonic analysis of the rocks involved in the main tectonic events? ii) what are the timing and relationships between these deformation events?

2. Regional Geological Framework

The CAOB of Inner Mongolia is subdivided into several, roughly W-E striking, litho-tectonic units namely, from south to north, the North China Craton, the Southern orogenic Belt (SOB), several microcontinents, including the Hunshandake block (HB), and the Hutag Uul block, the Northern orogenic Belt (NOB), and the Southern Margin of the Ergun block (SME) (Fig. 1; Xu et al., 2012).

2.1 The North China Craton (NCC)

The NCC is mainly composed of Archean trondhjemitic-tonalitic-granodiorite gneiss with mafic igneous rocks. Although the detailed tectonic evolution, timing and polarity of subduction remain disputed, it is now well accepted that the NCC was mainly built up during the Paleoproterozoic (ca. 2 Ga) by the collision of several Archean blocks (e.g. Zhao et al., 2005; Kusky and Li, 2003; Faure et al., 2007; Zhai et

al., 2010; Trap et al., 2012, and enclosed references). Undeformed Mesoproterozoic to Early Paleozoic, ca.10 km thick, sedimentary deposits intercalated with volcanic rocks unconformably cover the Paleoproterozoic belts (Zhang, et al 1999). All these rocks are in turn unconformably overlain by unmetamorphosed and weakly deformed Carboniferous-Permian strata. (BGMRIM. 1991; Hsü et al., 1991; Zhao et al., 2005; Kusky et al., 2007; Faure et al., 2007; Trap et al., 2007). Late Palaeozoic granite and granodiorite intrude into the Precambrian basement of the NCC (BGMRIM, 1991). The east-west striking Baiyan Obo-Chifeng fault is considered as the northern boundary between the NCC and the Bainaimiao arc that belong to the SOB (Shao, 1991; Tang, 1990; Tang et al., 1993; Xiao et al., 2003).

2.2 The South Orogenic Belt (SOB)

The SOB extends at least for more than 700km from the Tugurige area in the west via Ondor Sum to the Chifeng area in the east (Fig. 1). It is composed of the Ondor Sum mélange unit and the Bainaimiao arc unit (Xiao et al., 2003; Jian et al., 2008; Xu et al, 2012). The Ondor Sum mélange unit consists mainly of blocks of pillow basalts, gabbro, diabase, tuff, metasandstone, chert, pelagic sediments including iron-manganese formation, and rare limestone enclosed into a pelite-siltite matrix (Wang and Liu, 1986; Shao, 1991; Tang, 1990; Xiao et al., 2003). The Bainaimiao arc unit extends along an E-W trend from the Bater Obo in the west to the Chifeng in the east. It contains mainly andesite, basalt, a small amount of felsic lava, and volcanic-sedimentary rocks. Several granodiorite and granite plutons also crop out

(Xiao et al, 2003). Three magmatic phases have been identified from ca.500Ma to ca.415Ma (Jian et al., 2008). Based on the high initial strontium isotope ratio ($^{87}Sr/^{86}Sr$ = 0.7146) of granites and the εNd value of 2.4 ± 1.7 of granodiorite (Nie et al., 1999), Xiao et al., (2003) suggested that the Bainaimiao arc was formed by mixing between mantle-derived and crust-derived magmas emplaced in an active continental margin of Cordilleran-type.

2.3 The microcontinents

In southwestern Mongolia several microcontinents have been defined, namely the Hutag Uul block (Badarch et al., 2002), Totoshan Ulanul block (Yarmolyuk et al. 2005), and Tsagan Khairkhan block (Demoux, et al., 2009). They are dominated by quartz-rich micaschist, meta-volcanic rocks, meta-sandstones and marble (BGMRED, 1991). The Totoshan Ulanul Block contains metamorphic rocks dated at 952 ± 8Ma (single zircon U/Pb; Yarmolyuk et al. 2005; Demoux, et al., 2009). The Tsagan Khairkhan block yields ages of 916 ± 16Ma (Wang et al., 2001). In central Inner Mongolia, the existence of the Hunshandake Block was deduced from scattered outcrops of metamorphic rocks (BGMRIM, 1991) and the presence of Precambrian detrital zircon grains in mélange matrix (Xu et al., 2012). In our study area, Precambrian rocks are not exposed, however on the basis of microstructural analyses, we shall argue that the Hongqi mélange is underlain by a microcontinent, (cf. below). The correlation of this hypothetical microcontinent with the privious ones will be discussed in section 6.

3. The Hongqi area

3.1 The litho-tectonic units

The Hongqi study area is located in the north of Bayan Obo at the western end of the South Orogen of Inner Mongolia. Four litho-tectonic units are recognized from northwest to southeast, namely the Hongqi mélange, the Bainaimiao arc, an overlying sedimentary succession ranging from the Early Devonian to the Late Carboniferous, and the North China craton (Fig. 2).

3.1.1 The Hongqi mélange unit

To the north, the mélange rocks are hidden below the Mesozoic sedimentary rocks of the Erlian basin (Meng, 2003). To the south of the mélange unit, Permian magmatic rocks crop out. The entire mélange unit is cut into two parts by the Suji fault (Fig. 3A). The western part of the mélange is predominantly composed of fine grain quartzite, micaschist, sericite slate, siltstone, iron-bearing chert and metapelite with rare blocks of limestone. Coherent sedimentary strata of alternating beds of fine quartzite and metapelite are locally well preserved, suggesting a turbiditic origin for these rocks. The eastern part of the mélange exhibits a typical block-in-matrix structure. It mainly consists of tuffaceous siltstone, sericite chlorite schist, chlorite quartz schist, calc-slate, chert and a small amount of greywacke. Blocks include amphibolite, pillow basalt, volcanic rocks, limestone and chert(Fig.4A). These blocks display variable size ranging from tens of centimeters to several hundreds of meters. Mafic-ultramafic rocks, such as serpentinite, serpentinized peridotite and metagrabbro, are reported in the southern part

of the mélange (Jia et al., 2003). In the middle part of this unit, due to mining exploration work, amphibolite rocks are digged out below a greenschist cover.

Intense ductile shearing and mylonitization characterize all the rock types. To the south of the mélange, the available geological map shows Silurian strata composed of fossiliferous limestone and sandstone. However, our field observation indicates that these rocks are foliated, recrystallized, and contain elongated crinoids (Fig.4B and C). Additionally, those limestones are laterally discontinuous in the regional scale. Therefore, we consider these rocks as blocks within the Hongqi mélange.

The whole mélange unit is dominated by a greenschist-facies metamorphism with a common mineral assemblage of chlorite, muscovite, biotite, plagioclase and quartz in the metapelite. The amphibolite blocks contain metamorphic minerals such as hornblend, plagioclase, epidote and quartz, indicating an amphibolite facies metamorphism. In the western part of the mélange, biotite and andalusite grains, oblique to the regional foliation, are related to a contact metamorphism probably due to plutonic intrusions emplaced after the main deformation. Graptolite fossils assigned to *Callograptus* sp., *Desmograptus* sp., and *Dictyonema* sp., found in the tuffaceous rocks, suggest an Early to Middle Ordovician age (BGMRIM, 1991). An acidic metavolcanite block is dated at 485 ± 14 Ma by ICP-MS on zircon (see Section 5).

3.1.2 The Bainaimiao arc

Eastward of the mélange, in the Bater Obo area, crops out the Bainaimiao arc. It is composed of basalt, basaltic andesite, andesite, interbedded with up to 10-20 m of

tuffaceous siltstone as well as agglomerate, pyroclastite and volcanic breccia. The

basalts contain three types of aphanitic, porphyritic and vesicular structure. The basalts

with typical porphyritic textures contain olivine (3-5%), pyroxene (10-15%) and

feldspar (25-30%) phenocrysts embedded in a fine-grained groundmass of glass,

plagioclase and pyroxene microcline. Secondary chloritic and sericitic alterations and

fine carbonate veins are common in the volcanic rocks. Numerous granite,

plagiogranite, granodiorite, quartz diorite and diorite plutons with calc-alkaline

geochemical signatures are exposed (Xu and Tao, 2003). Jian et al., (2008) suggested

that the quartz diorites are high-K calc-alkaline rocks with adakitic feature, indicating

an island arc setting. The age of those plutons with arc signature is about 440~460Ma

(Jian et al., 2008; Li et al., 2010; Fig. 2).

3.1.3 The overlying sedimentary succession

The Early Devonian and Late Carboniferous rocks unconformably overly the volcanic,

sedimentary and plutonic rocks mentioned in the previous section. The Lower

Devonian Chaganhabu Formation (IMBGMR, 2002), exposed in the southern part of

the Hongqi mélange and the Bainaimiao arc, can be subdivided into two units. The

lower unit, with a thickness of ca.975m, consists of basal red conglomerate, siltstone,

grey arkose, upperwardly reef limestone and red quartzose arkose and micrite. The

upper unit is composed of turbiditic deposits with a thickness of ca.1500m (Zhang et

al., 2004). The association of various fossils, such as corals, brachiopods, bryozoan and

conodonts in the limestones indicate an Early Devonian age. The conglomerate and

terrigeneous rocks unconformably cover the Upper Silurian series with an angular

unconformably (IMBGMR, 2002; Zhang et al., 2004). Our observation of the basal

conglomerates of the lower Devonian sequence reveals pebbles of volcanic rock,

metamorphic rock, quartzite and chert (Fig. 4B, C and D). The unconformable contact

of this sequence above the underlying deformed limestone rocks can be observed as

well. The Uppermost Carboniferous strata consist of fossiliferous limestone and clastic

rocks that unconformably cover the lower Devovian (IMBGMR, 2002). This Early

Devonian to Late Carboniferous sedimentary succession did not experienced a ductile

or synmetamorphic deformation, but only folding and brittle faulting.

3.1.4 The North China Craton basement

The southernmost unit of the study area is occupied by Meso-to Late Proterozoic

volcanic-sedimentary series (Bayan Obo group; Fig. 2). These unmetamorphosed

sedimentary rocks represent the NCC basement in the study area.

3.2 The bulk architecture of the Hongqi area

A general cross section of the Hongqi area is drawn along a SW-NE strike (Fig.

3B). The regional framework is represented by an antiform composed of several

SE-NW striking folds with hectometer-wavelength. In the centre of the antiform, a

bimodal volcanic rock with associated gabbro and Early Triassic tonalitic pluton

superimpose on the Hongqi mélange unit. The mélange is unconformably covered to

the south by the Early Devonian red sandstone, and to the north by Late Carboniferous

limestone. The Early Devonian rocks, gently dipping to the west, do not display any metamorphism or ductile deformation. The structural characteristics of the mélange are described in detail below.

3.3 Microstructural analysis of the Hongqi mélange

From our field observations, three deformation events namely: D_1, D_2 and D_3, with the first two of ductile and syn-metamorphic style, and the third one of gentle folding, are recognized.

The D_1 event is responsible for the formation of the main foliation (S_1), stretching lineation (L_1) and intrafolial fold (F_1). In the field, S_1 is defined by the alternation of chlorite quartz schists and sericite chlorite schists. The L_1 lineation is marked by elongated clasts, quartz ribbons, aggregates of chlorite and mica (Fig. 5A). Intrafolial F_1 folds with axes plunging to the SE are also developed within the S_1 foliation (Fig. 5B). In places, the S_1 foliation is approximately parallel to the sedimentary bedding, which is well preserved in the metapelite and meta-quartzstone. Pinch-and-swell and boudinaged structures are also observed in quartz schists indicating a layer-parallel shearing (Fig. 5C). At the microscopic scale, pressure solution seams of dark insoluble material and aligned recrystallized phyllosilicates represent S_1 (Fig. 6A). The S_1 foliation mostly dips to the NE or SW due to D_3 folding. The well foliated and lineated blocks wrapped around by S_1 matrix foliation display SE-NW directed elongation. The L_1 lineation in amphibolite blocks is represented by oriented hornblende and recrystallized quartz and plagioclase aggregates (Fig. 6B). Pillow lava blocks, up to

30-50 cm in diameter, are also elongated in the NW-SE direction (Fig. 5D). Sandstone blocks exhibit commonly elongated chert pebbles along the NW-SE direction. Limestone blocks display aligned and elongated crinoids along the NW-SE stretching direction of L_1.

The D_2 event is associated with the development of NW-verging asymmetrical folds (F_2) that deform S_1 and L_1. The most striking structure is meter-scale asymmetrical fold F_2. F_2 fold with NE-SW trending subhorizontal axes (L_2) exhibits a NW vergence (Fig. 5E). Asymmetric kink bands, bending the S_1 foliation and L_1 mineral lineation, are well developed in quartz sericitic schists (Fig. 5F).

The D_3 event is represented by NW-SE trending upright folds (F_3) responsible for the bulk architecture of the area. Although the eastern and western parts of the mélange unit on each side of the Suji fault should have experienced similar structural histories, the structures of the western part are, to some degree, disturbed by the activity of the brittle Suji fault as well as the post-tectonic intrusions (Figs. 3C and 3D). In contrast, the three deformation events are well recognized in the eastern part (Figs. 3A, 3E and 3F).

The D_3 event is defined by SE-NW striking upright folds. Similar folds are widespread in the layers where incompetent material dominates such as chlorite schists (Fig. 5G), whereas parallel folds with SE-NW trending axes develops in the quartz sandstone layers (Fig. 5H). At the macroscopic scale, F_3 folds deform the S_1 foliation, giving rise to the general antiformal structural framework of the Hongqi mélange (Figs. 3B and 3E).

Thin sections, made parallel to L_1 and perpendicular to S_1, exhibit numerous kinematic indicators. In amphibolite blocks, the recrystallized amphibole and quartz aggregates indicate a top-to-WNW shearing (Fig. 6B). In mylonitic volcanic-sedimentary rocks, asymmetric pressure shadows defined by chlorite fibers around feldspar porphyroclasts indicate a top-to-the-NW sense of shear (Figs. 6C and 6D). Quartz oblique grain shape fabric showing a top-to-the NW shearing is also recognized (Fig. 6E). Boudins formed by pull-apart clasts with chlorite aggregates filling in the cracks suggest a top-to-the-NW sense of shear (Fig. 6F). Mica fishs,and shear bands developed in the metapelites also have the same sense of shear (Fig. 6G). Sigma-type porphyroclast systems in the metapelite in the western part of the mélange exhibit a top-to-the-N thrusting (Fig. 6H). Thus the kinematic criteria of the mélange unit show a consistent top-to-the-NW sense of shear.

In summary, the Hongqi mélange of block-in-matrix structure experienced three phases of deformation. The D_1 phase is dominated by a consistent top-to-the-NW sense of shear coeval with the mélange formation. The NW-verging asymmetric folds developed during the D_2 event can be interpreted as the continuation of the same ductile shearing under less penetrative conditions. The last D_3 deformation forms upright folds, which control the general structural framework of the mélange unit. The Early Devonian red sandstone unconformably covering this mélange unit does not record the D_1 and D_2 events, and thus provides an upper time limit for the termination of the ductile events. The km-scale upright folding involves the Devonian and Carboniferous rocks.

4. The Ondor Sum area (Fig. 7)

4.1 The litho-tectonic units

In the Ondor Sum area, two litho-tectonic units are recognized from north to south. The geometrically lowermost unit corresponds to the Ondor Sum mélange, it is bounded to the south by an amphibolite-granite unit, called "Tulinkai ophiolite" (Jian et al., 2010).

4.1.1 The Ondor Sum mélange unit

The Ondor Sum mélange crops out in three places: the southern one (or Ulan Obo-Tulinkai area), the middle and the northern Ulan valley areas (Fig. 7A). The Ondor Sum mélange is mainly composed of sericite quartz schists, chlorite-epidote schists and albite-chlorite-epidote schists. Various decimeter to several meter sized lenses of sandstone, limestone, mafic rocks and iron-bearing quartzite are scattered into a greenish matrix. These green and red blocks dispersed in a sandy-silty matrix define a typical coloured mélange formation (Figs. 8A and B). Two types of basalts are recognized near the Ulan valley. One is represented by flattened vesicular basalt. As described by Xiao et al. (2003), the pillow lavas are up to 30-50 cm in diameter, elongated, facing upward, and dipping to the north. The other type of basalt is undeformed, with a vesicular or massive texture filled by centimeter sized white quartz. These deformed pillow basalts are blocks within the mélange and were geochemically interpreted as originated from a sea-mount (Huang et al., 2006). They must not be

confused with undeformed basalts that occupy the top of some hills. Some of these undeformed basalts yield a radiometric age of 260Ma (Miao, 2007); Cenozoic basalts are also likely (IMBGMR, 1976).

In the Ondor Sum mélange, the rocks are pervasively deformed, mylonitized and metamorphosed into greenschist or blueschist facies. Petrological study of metamorphic assemblages led previous authors to deduce P-T conditions of the blueschist facies rocks at 7-8Kb and 380-400ºC, respectively (Tang et al., 1992). Glaucophane from blueschists yields $^{40}Ar/^{39}Ar$ ages of 446 ± 15 Ma and 426 ± 15Ma (Xiao et al., 2003; and references therein). Phengite from quartzite mylonites at Ondor Sum has $^{40}Ar/^{39}Ar$ plateau age of 449-453Ma (De Jong, et al., 2006). In agreement with Xiao et al. (2003), we consider that this rock assemblage, derived of Fe and Mn siliceous sediments, volcaniclastic sediments, basalts and spilites, indicates an ocean floor origin.

4.1.2 The Tulinkai unit

The Tulinkai unit spreads in the E-W direction from Tulinkai to Ulan Obo (Fig. 7A). In the literature, the Tulinkai unit is described as an "ophiolitic suite" (Hu et al., 1990; Jian et al., 2010). Our field observations indicate that the dominant rock is coarse to medium grained, well foliated amphibolite, diorite and gabbro. Granitic layers are also widespread. Some appear as dykes cross cutting the foliation and others show foliation parallel veins (Figs. 8C and 8D). Large volumes of diorite and granodiorite with mafic boudins are exposed further south of the "ophiolitic" rocks. Cumulate

gabbros from Tulinkai have a zircon SHRIMP age of 457±4Ma, and a diorite intrusion with an adakitic geochemical signature has a zircon age of 467±6Ma (Liu et al., 2003; Miao et al., 2007). These rocks have been interpreted as supra-subduction zone type ophiolite (Liu et al., 2003; Jian et al., 2008). However, from our field observation, usual ophiolitic component, such as serpentinized peridotite, pillow basalts and siliceous sediments, are not observed. Therefore, in the following section, we shall argue that these rocks might belong to the deep part of a magmatic arc.

4.2 The bulk architecture

Based on field structural measurements, the bulk architecture of the Ondor Sum area is dominated by a NE-SW trending antiform (Fig. 7B). The general structure results of a polyphase deformation evolution. The southern limb of the antiform is dominated by a steeply south dipping or vertical foliation (Fig. 7C). In the middle part, the main foliation is involved in a series of nearly E-W trending upright folds (Fig. 7D). The Ulan valley, dominated by northwest dipping foliation, corresponds to the northern limb of the antiform. To the south of the Ondor Sum mélange, the Tulinkai unit is fault-contact with the mélange unit. A top-to-the-north thrusting is documented (IMBGMR, 1976). The light colored gneiss-amphibolite alternation of the Tulinkai unit is ductilely deformed. Amphibolitic and granitic dykes commonly form meter-scale isoclinal folds with approximately NW-dipping axes. The northward and southward dip of the Carboniferous limestone bedding, in the northern and southern limbs of the Ondor Sum antiform indicate that the last deformation event took place after the

Carboniferous. However, the synmetamorphic deformations are clearly older than the deposition of the Carboniferous series.

4.3 Microstructural analysis

Like the Hongqi area, three deformation events are also identified in the Ondor Sum area. They are named here D_1, D_2 and D_3, nominally like in the Hongqi area but with a slightly different meaning for D_3.

In the southern limb of the mélange unit, the approximately E-W trending S_1 is subvertical or dipping at a high angle to the south. The L_1 subvertical lineation is represented by elongated quartz, feldspar or calcite clasts, and chlorite fibers on the S_1 surface (Fig. 8E). In thin section, the lineation is marked by oriented phyllosilicates and recrystallized carbonate clasts within insoluble material. For this part, a subhorizontal crenulation lineation is weakly developed. But centimeter- to meter- scale asymmetric folds are observed in the chlorite quartz schistose layers. Shear criteria, such as pressure shadows, sigma type porphyroclast systems and shear bands indicate a SE (or S) moving upward sense of shear (Figs. 10A, 10B and 10C). Thus, when the foliation is rotated to horizontal, the kinematic indicators are top-to-the-NW (or N) sense of shear.

In the central part of the Ondor Sum area, a series of E-W striking centimeter- to millimeter-scale upright folds deforming S_1 are identified. Both the chlorite and sericite schist matrix and the blocks exhibit a N-S to NW-SE stretching lineation (L_1) marked by elongated recrystallized quartz and chlorite aggregates. Along the lineation, pressure shadows and sigma-type porphyroclasts indicate a top-to-the-NW sense of shear when

S_1 lies subhorizontal or gently tilted (Fig. 10D). S_2 is characterized by centimeter wavelength crenulations. At the microscope scale, a S_3 subvertical cleavage cuts at a high angle the S_1 foliation (Fig. 10E).

The Ulan valley has been studied in detail since it is well exposed (Wang and Liu, 1986; Xiao et al., 2003; Fig.9A). At the southern entrance of the Ulan valley, S_1, generally N-S striking, contains a nearly E-W striking L_1 mineral lineation. However, when moving northward, S_1 turns to an E-W strike and dips to north or northwest. A conspicuous NW-SE trending stretching and mineral lineation is preserved on the gently dipping foliation (Figs. 8F and 9B). Crenulation wrinkles and asymmetric microfolds (F_2) that intensively deform the S_1 foliation and L_1 lineation are commonly developed (Figs. 8G and H). F_2 folds are scattered with subhorizontal axes (Fig.9B). An axial planar crenulation cleavage (S_2) marked by the opaque material is well developed (Fig. 10F). S_2 cleavage is tilted to the northwest due to the D_3 antiformal upright folding. Locally, the intense F_2 folding gives rise to well developed inverted limbs with some F_2 folds apparently overturned to the SE (Fig. 8H). In thin sections cut parallel to the L_1 lineation, asymmetric pressure shadows and sigmoidal porphyroclasts indicate a top-to-the-NW sense of shear (Figs. 10G and 10H).

In conclusion, the Ondor Sum mélange unit is a terrigenous volcaniclastic block-in-matrix series with blocks of oceanic origin. It experienced three deformation phases: D_1 was responsible for the S_1 foliation and L_1 stretching lineation coeval with a greenschist facies metamorphism. Taking S_1 as a reference surface, two subsequent deformation events, D_2 and D_3 are recognized. The D_2 event associated with the F_2

asymmetric folds can be interpreted as the continuation of the top-to-the-NW shearing, that occurred by shortening at a low angle or subparallel to S_1. After the deposition of the Late Carboniferous limestone, the D_3 event gave rise to the general antiform to form the regional structural framework.

5. Geochronological constraints

New zircon dating is obtained by ICP-MS U-Pb analyses method. Cathodoluminescence (CL) images were performed by CAMECA SX-50 microprobe at Peking University in order to document zircon internal structures. Zircon laser ablation ICP-MS U-Pb analyses were conducted on an Agilent 7500a ICP-MS equipped with a 193 nm laser in China University of Geosciences, Beijing. Laser spot size was set to ~36μm for analyses, laser energy density at 8.5 J/cm^2 and repetition rate at 10 Hz. Isotopic ratios and element concentrations of zircons were calculated using GLITTER (ver. 4.4, Macquarie University). Concordia ages and diagrams were obtained using Isoplot/Ex (3.0, Ludwig, 2003). The common lead was corrected using LA-ICP-MS Common Lead Correction (ver. 3.15), following the method of Andersen (2002). The summarized age data and our new measured isotopic data are given in Tables 1 and 2.

An acidic volcanite block (Sample 090716-29; located at 42º59´24″N, 109º 55´20″ E) embedded in the Hongqi mélange was dated. In thin section, the sample shows a mylonitic texture, with feldspar clasts surrounded by elongated recrystallized subgrain quartz aggregates. Most of the zircon grains from the acidic volcanite

(090716-29) are weakly luminescent, and surrounded by a thin bright luminescent rim (Fig. 11A). Some analyzed spots have low Th/U ratios, generally close to 0.1. A few U-Pb isotopic compositions are discordant (Table 2), probably due to Pb loss during shearing in the mélange. 14 of 20 analyzed spots plot slightly on the right side of the Concordia curve, and define three populations around ca. 560~590 Ma, ca. 510-540Ma, and 485 ± 14Ma (n=4; Fig. 11B).

Our analysis paid much attention to detect youngest ages of the volcanite, thus spots focus on zircon rim. The low Th/U (<0.1) ratio, a common geochemical feature of high-grade metamorphic zircons (Williams et al., 1996), are present in both younger and older populations (Table 2). It is worth noting that no distinct high-grade metamorphic minerals are observed in thin section. Globally, the mélange unit experienced a green schist facies metamorphism. Therefore, we consider that these zircons are magmatic ones possibly slightly suffering metamorphism. The youngest population at 485 ± 14Ma represents the age of the acidic volcanism.

6. Discussion

6.1 Deformation comparison between the Hongqi and Ondor Sum areas

During our field work, we did not find HP rocks, all the microstructures described in this paper are coeval with a greenschist facies metamorphism. The three phases of deformation of the Ondor Sum mélange can be roughly compared with those of the Hongqi mélange as follows: 1) the main event, D_1, is responsible for the development of the S_1 foliation, NW-SE striking stretching lineation (L_1), and intrafolial folds (F_1)

with axes parallel to L_1. In the Hongqi area, D_1 is coeval with a green schist facies metamorphism whereas, in the Ondor Sum area blue schist facies relicts, such as glaucophane, phengite are locally preserved (Tang et al., 1993; De Jong et al., 2006). Our kinematic observations show a top-to-the-NW sense of shear in both study areas. F_1 folds corresponding to a-type folds formed during the ductile shearing in the Hongqi area. The D_1 structural elements are subsequently deformed by the D_2 event represented dominantly by numerous NW-verging asymmetric folds associated with an axial-planar crenulation cleavage (S_2). Due to the subsequent deformation (D_3), S_2 dips to either the SE or the NW in the Ondor Sum area whereas, dips to the NE or the SW in the Hongqi area. The blueschist and quartz mylonites with age ranging from 453 to 426Ma (Tang et al., 1993; De Jong et al., 2006) recorded the Ondor Sum subduction event. In the Hongqi area, the deformed Late Silurian fossiliferous limestone blocks mark the youngest age of the Hongqi mélange.

6.2 Crustal scale structure framework

A N-S oriented interpretative crustal scale cross section is proposed on the basis of structural, lithological and geochronological data presented above (Fig. 12). The Early Paleozoic Hongqi mélange belt, is unconformably overlain by the Early Devonian red sandstone and Late Carboniferous limestone.

The mélange belt displays a top-to-the-NW thrusting, indicating a southeastern oceanic subduction. The volcanic rocks exposed in the Bater Obo area are comparable with the rocks in the Bainaimiao area. The mafic plutonic rocks exposed in the Tulinkai

unit might represent the deep plutonic part of the Bainaimiao arc. The age of the volcanite block dated in the Hongqi mélange, similar to those of the Bainaimiao arc suggest that the magmatic blocks in the mélange might derive from the arc rocks of the upper plate.

At depth, a possible crustal basement is inferred here on the basis of the following points. Firstly, in order to terminate the oceanic subduction before Early Devonian, some buoyant material, such as huge seamount, large oceanic plateau, or microcontinent, underneath the Hongqi mélange, is needed. The collision of this feature will allow the oceanic subduction and the coeval arc magmatism to stop. Secondly, Precambrian crystalline basement rocks are recognized, in the Hutag Uul terrane (Badarch et al., 2002), Totoshan Ulanul block (Yarmolyuk et al. 2005; Demoux, et al., 2009), Tsagan Khairkhan massif (Wang et al., 2001) and Hunshandake microcontinent (Xu et al., 2012). Precambrian middle to high grade metamorphic paragneiss are also recognized in the north of the Ondor Sum, near Sunityouqi (Fig. 1; BGMRIM, 1991; Hsu et al., 1991; Li et al., 1995; Zhang et al., 1999) or in the Xilingele (or Xinlin Gol) complex near Xilinhot (Zhu et al., 2004). Though an oblique subduction of the underlying plate, accommodated by strike-slip faulting can be proposed to terminate a subduction (Choulet, 2012), in the study area, no strike-slip fault of Early Paleozoic age, and associated ductile deformation are observed. Therefore, we argue that the structural features presented above, and particularly the syn-metamorphic ductile shearing can be explained by the subduction of a microcontinent below the North China block.

6.3 A possible geodynamic evolution model

On the basis of our geological data presented in the previous sections, a possible Early Paleozoic geodynamic scenario for the evolution of the eastern part of the CAOB in Inner Mongolia is proposed here.

The Ordovician to Silurian Subduction: An Early Paleozoic SE-dipping Paleo-Asian Ocean subduction zone developed along the northern margin of North China Craton from the Hongqi to the Ondor Sum area. It is supported by the consistent top-to-the-NW sense of shear indicators. This oceanic subduction gave rise to the Bainaimiao magmatic arc, and the Hongqi and Ondor Sum mélange units (Fig. 13A). Both the Hongqi and the Ondor Sum areas experienced two ductile deformation phases before the Early Devonian. Moreover, the north dipping schists at the Ulan valley, which constitute the northern limb of the antiform, show a top-to-the NW sense of shear that is unconsistent with a Precambrian northward subduction.

The Late Silurian Collision: The collision likely occurred in Late Silurian, since the Early Devonian red sandstones unconformably cover the Hongqi mélange. Moreover, the basal conglomerates of the Early Devonian sediments contain pebbles of the underlying litho-tectonic units. Accretionary tectonics and magmatism must have been stopped at that time. This scenario is supported by the undeformed pegmatite of $411\pm8Ma$ that cuts the low P/T metamorphic complex in the Bainaimiao area (Zhang et al., 2012), and the ca. 417Ma tonalite interpreted as due to collision magmatism near the Hongqi area (Jian et al., 2008). Subsequently, a Late Carboniferous platform limestone developed in a vast area, extending throughout the eastern part of Inner

Mongolia (BGMRIM, 1991). In our study area, the most likely is that a microcontinent, entered in the trench and collided with the Andean active margin of the North China Craton (Fig. 13B). This hypothetical microcontinent might be connected with the South Gobi microcontinent (Sengor and Natal'in, 1996) or the Hunshandake block (Xu et al., 2012). But, the size and distribution of this hypothetic microcontinent are not documented yet, and the correlations with other microcontinental blocks between North China Craton and Siberia remains hypothetic.

7. Conclusion

i) The mélange belt exposed in the Hongqi and Ondor Sum areas, is characterized by two phrases of ductile deformation and a top-to-the-NW sense of shear, suggesting a southeastward subduction during the Early Paleozoic.

ii) The ductile deformations in the Ondor Sum-Hongqi mélange belt are coeval with greenschist facies metamorphism. The unconformably overlying Early Devonian sedimentary rocks indicate that subduction and collision should terminate before the Early Devonian.

iii) In the present knowledge, the South-directed of a microcontinent below the North China Craton appears as the most likely geodynamic scenario to account for the structural evolution.

References:

Andersen, T., 2002. Correction of common lead in U-Pb analyses that do not report ^{204}Pb, Chemical Geology 192, 59–79.

Badarch, G., Cunningham, W.D., Windley, B.F., 2002. A new terrane subdivision for Mongolia: implications for the Phanerozoic crustal growth of Central Asia. Journal of Asian Earth Sciences 21, 87–104.

BGMRIM (Bureau of Geology and Mineral Resources of Inner Mongolia), 1991.Regional Geology of NeiMongol (Inner Mongolia) Autonomous Region.

Geological Publishing House, Beijing (in Chinese with English summary).

Cawood, P., Kröner, A., Collins, W.J., Kusky, T., Mooney, W.D., Windley, B.F., 2009. Accretionary orogens through Earth history, in Cawood P., and Kröner A. (Eds.), Earth Accretionary systems in space and time. Geological Society Special Publication, 318, 1-36.

Chen, B., Jahn, B.M., Tian, W., 2009. Evolution of the Solonker suture zone: Constrains from zircon U-Pb ages, Hf isotopic ratios and whole-rock Nd-Sr isotope compositions of subduction and collision-related magmas and forearc sediments. Journal of Asian Earth Sciences 34, 245-257.

Chen, C., 2011. geochronology, geochemistry, and its geological significance of the Early Permian volcanic rocks in Damaoqi, Inner Mongolia. Master degree thesis, Peking University. 50pp.

Chen, C., Zhang, Z.C., Guo, Z.J., Li, J.F., Feng, Z.S., Tang, W.H., 2012. Geochronology, geochemistry, and its geological significance of the Permian Mandula mafic rocks in Damaoqi, Inner Mongolia. Science China earth Sciences 55, 39-52.

Choulet, F., Faure, M., Cluzel, D., Chen, Y., Wei, L., Wang., B., 2012. From oblique accretion to transpression in the evolution of the Altaid collage. Gondwana Research 21,

530-548.

Condie, K.C., 2007. Accretionary orogens in space and time. In Hatcher R.D. Jr., Carlson, M.P., Mc Bride J.H., Martinez-Catalan, J.R., 4D framework of the continental crust. Geological Society of America Memoir 200, 154-158.

De Jong, K., Xiao, W.J., Windley, B.F., Masago, H., Lo, C.H., 2006. Ordovician $^{40}Ar/^{39}Ar$ phengite ages from the blueschist-facies Ondor Sum subduction-accretion complex (Inner Mongolia) and implications for the early Paleozoic history of continental blocks in China and adjacent areas. American journal of Science 306 799-845. DOI 10.2475/10.2006.02.

Demoux, A., Kröner, A., Liu, D.Y., 2009. Precambrian crystalline basement in southern Mongolia as revealed by SHRIMP zircon dating. International Journal of Earth Sciences (Geol Rundsch) 98, 1365-1380. DOI 10.1007/s0051-008-0321-4.

Faure, M., Trap, P., Lin, W., Monié, P., Bruguier, O., 2007. Polyorogenic evolution of the Paleoproterozoic Trans-North China Belt, new insights from the in Lüliangshan-Hengshan-Wutaishan and Fuping massifs. Episodes 30, 96-107.

Frey, M., 1987. Very low-grade metamorphism of clastic sedimentary rocks. in: Low Temperature Metamorphism (M. Frey, editor). Blackie, Glasgow and London, 9-58.

Hsü, K. J., Wang, Q., Li, J., Hao, J., 1991.Geologic evolution of the Neimonides: A working hypothesis. Eclogae Geologicae Helvetiae 84, 1 – 31.

Hu, X., Xu, C.S., Niu, S.Y., 1990. Evolution of the Early Paleozoic Continental Margin in Northern Margin of the North China Platform. Peking University Publish House, Beijing. (in Chinese with English abstract).

Huang, J.X., Zhao, Z.D., Zhang, H.F., Hou, Q.Y., Chen, Y.L., Zhang, B.R., Depaolo, D.J., 2006. Elemental and Sr-Nd-Pb isotopic geochemistry of the Wenduermiao and Bayanaobao-Jiaoqier ophiolites, Inner Mongolia: Constraints for the characteristics of the mantle domain of eastern Paleo-Asian Ocean. Acta Petrologica Sinica 22,2889-2900.

IMBGMR, 1976 .Regional Geological Investigation Report of 1:200000 scale Xianghuangqi Quadrangle. Inner Mongolian Bureau of Geology and Mineral Resources.

IMBGMR, 2002 .Regional Geological Investigation Report of 1:250000 scale BaiyunObo Quadrangle. Inner Mongolian Bureau of Geology and Mineral Resources.

IMBGMR, 2008 .Regional Geological Investigation Report of 1:50000 scale

Wulanbulage Quadrangle. Inner Mongolian Bureau of Geology and Mineral Resources

Jahn, B.M., 2004. The Central Asian Orogenic Belt and growth of the continental crust in the Phanerozoic. In: Malpas, J., Fletcher, C.J.N., Ali, J.R., Aitchinson, J.C., (Eds.), Aspects of the Tectonic Evolution of China. Geological Society, London, pp 3–100.

Jia, H.Y., Baoyin, W.L.J., Zhang, Y.Q., 2003. Characteristics and tectonic significance of the Wude suture zone in northern Damaoqi, Inner Mongolia. Journal of Chengdu University of Technology (Science & Technology edition) 30, 30-34. (In Chinese with English abstract).

Jian, P., Liu, D.Y., Kröner, A., Windley, B. F., Shi, Y.R., Zhang, F.Q., Shi, G.H., Miao, L.C., Zhang, W., Zhang, Q., Zhang, L.Q.,Ren, J.S., 2008. Time scale of an early to mid-Paleozoic orogenic cycle of the long-lived Central Asian Orogenic Belt, Inner Mongolia of China: Implications for continental growth. Lithos 101, 233-259.

Jian, P., Liu, D.Y., Kroner,A., Windley, B.F., Shi, Y.R., Zhang, W., Zhang, F.Q., Miao, L.C., Zhang, L.Q., Tomurhuu, D., 2010. Evolution of a Permian intraoceanic arc–trench system in the Solonker suture zone, Central Asian Orogenic Belt, China and Mongolia. Lithos 118, 169-190.

Kusky T.M.,Windley, B., Zhai, M., 2007, Tectonic evolution of the North China Block:

from orogen to craton to orogen. In: Zhai, M., Windley, B., Kusky, T., Meng, Q.(Eds.),

Mesozoic sub-continental lithospheric thinning under eastern Asia. Geological

Society, London, Special Publications 280, 1-34.

Kusky, T. M. Li, J. H., 2003. Paleoproterozoic tectonic evolution of the North China

Craton. Journal of Asian Earth Science 22, 383-397.

Li, J.F., Zhang, Z.C., Han, B.F., 2010. Ar-Ar and zircon SHRIMP geochronology of

hornblendite and diorite in northern Darhan Muminggan Joint Banner, Inner Mongolia,

and its geological significance. Acta Petrologica et Mineralogica 29, 732-740. (In

Chinese with English abstract).

Li, S.J., Gao, D.Z., 1995. New discovery of geological structures in Sonid Zuoqi of

Inner Mongolia and discussion on tectonic features. Journal of Graduate School, China

University of Geosciences 9, 130-141. (In Chinese with English abstract).

Liu, D.Y., Jian, P., Zhang, Q., Zhang, F.Q., Shi, Y.R., Shi, G.H., Zhang, L.Q., Tao, H.,

2003. SHRIMP Dating of Adakites in the Tulingkai Ophiolite, Inner Mongolia:

Evidence for the Early Paleozoic subduction. Acta Geologica Sinica 77, 317-327. (In

Chinese with English abstract).

Ludwig, K.R., 2003. User's Manual for Isoplot 3.0: A Geochronological Toolkit for

Microsoft Excel Berkeley Geochronology Center. Special publication 4, 1–71.

Meng, Q.R., 2003. What drove late Mesozoic extension of the northern China-Mongolia tract? Tectonophysics 369, 155-174.

Miao, L.C., Zhang, F.Q., Fan, W.M., Liu, D.Y., 2007. Phanerozoic evolution of the Inner Mongolia-Daxinganling orogenic belt in North China: constraints from geochronology of ophiolites and associated formations. In: Zhai MG, Windley BF, Kusky TM, Meng QR (eds), Mesozoic Sub-Continental Lithospheric Thinning Under Eastern Asia. Geological Society, London, Special Publication 280, 223–237.

Nie, F.J., Bjørlykke, A., 1999. Nd and Sr isotope constraints on the age and origin of Proterozoic meta-mafic volcanic rocks in the Bainaimiao-Wenduermiao district, south-central Inner Mongolia, China. Continental Dynamics 4, 1-14.

Sengor, A.M.C., Natal'in, B.A., Burtman, V.S., 1993. Evolution of the Altaid tectonic collage and Paleozoic crustal growth in Eurasia. Nature 364, 299-307.

Sengor, A.M.C., Natal'in, B.A., 1996. Paleotectonics of Asia:Fragments of a synthesism. In: Yin, A., Harrison, T.M. (Eds.), The Tectonic Evolution of Asia, Cambridge University Press, New York, pp.486-640.

Shao, J.A., 1991.Crustal Evolution in the Middle Part of the Northern Margin of the Sino-Korean Plate, Peking University Publish House, Beijing (in Chinese with English abstract).

Tang, K., 1990. Tectonic development of Paleozoic fold belts at the north margin of the Sino-Korean craton, Tectonics 9, 249-260.

Tang, K.D., 1992. Tectonic evolution and minerogenetic regularities of the fold belt along the northern margin of sino-korean plate. Peking University Publishing House, Beijing (in Chinese with English abstract).

Tang, K.D., Yan Z.Y., 1993.Regional metamorphism and tectonic evolution of the Inner Mongolian suture zone. Journal of Metamorphic Geology 11, 511 – 522.

Trap, P., Faure, M., Lin, W., Monié, P., 2007. Late Palaeoproterozoic (1900–1800Ma) nappe stacking and polyphase deformation in the Hengshan-Wutaishan area: implication for the understanding of the Trans-North China Belt, North China Craton. Precambrian Research 156, 85–106.

Trap, P., Faure, M., Lin, W., Le Breton, N., Monié, P., 2012. Paleoproterozoic tectonic evolution of the Trans-North China Orogen: Toward a comprehensive model. Precambrian Research 222-223, 450-473.

Wang, Q., Liu, X.Y., 1986. Paleoplate tectonics between Cathaysia and Angaraland in Inner Mongolia of China. Tectonics 5, 1073-1088.

Wang, T., Zheng,Y.D., Gehrels, G.E., Mu,Z.G., 2001. Geochronological evidence for existence of South Mongolian microcontinent zircon U-Pb age of grantoid gneisses from the Yagan-Onch Hayrhan metamorphic core complex. Chinese Science Bulletin 46, 2005-2008.

Williams, I.S., Buick, I.S., Cartwright, I., 1996. An extended episode of early Mesoproterozoic metamorphic fluid flow in the Reynolds Range, central Australia. Journal of Metamorphic Geology 14, 29–47.

Windley, B.F., Alexeiev, D., Xiao, W.J., Kröner, A., Badarch, G, 2007. Tectonic models for accretion of the Central Asian Orogenic Belt. Journal of the Geological Society, London 164, 31-47.

Xiao,W.J.,Windley, B.F., Hao, J., Zhai,M., 2003. Accretion leading to collision and the Permian Solonker suture, Inner Mongilia, China: termination of the Central Asian Orogenic Belt. Tectonics 22, 1069. doi:10.1029/2002TC001484.

Xiao,W.J., Han, C., Yuan, C., Sun, M., Lin, S., Chen, H., Li, Z., Li, J., Sun, S., 2008.

Middle Cambrian to Permian subduction-related accretionary orogenesis of northern Xinjiang, NW China: implications for the tectonic evolution of central Asia. Journal of Asian Earth Sciences 32, 102-117.

Xu, B., Charvet, J., Chen, Y., Zhao, P., Shi, G.Z., 2012. Middle Paleozoic convergent orogenic belts in western Inner Mongolia (China): framework, kinematics, geochronology and implications for tectonic evolution of the Central Asian Orogenic Belt, Gondwana Research, doi:10.1016/j.gr.2012.05.015

Xu, B., Chen, B., 1993. The opposite subduction and collision between the Siberian and Sino-Korean plates during the early-middle Paleozoic. Report No: 4 of the IGCP Projrct 283: Geodynamic Evolution of Paleoasian Ocean, Novosibirsk, USSR, pp.148-150.

Xu, B., Chen, B., 1997. Framework and evolution of the middle Paleozoic orogenic belt between Siberian and North China Plates in northern Inner Mongolia. Science in China (Series D) 40, 463-469.

Xu, B., Charvet, J., Zhang, F.Q., 2001. Primary study on petrology and geochronology of the blueschist in Sonid Zuoqi, northern Inner Mongolia. Chinese Journal of Geology 36, 424–434 (in Chinese with English abstract).

Xu, L.Q., Tao, J.X., 2003. Characteristics and tectonic signification of Ordovician granites in northern Damao, Inner Mongolia. Geology and Mineral Resources of South China 01, 17-22. (In Chinese with English abstract).

Yan, Z.Y., Tang, K.D., Bai, J.W., Mo, Y.C., 1989. High pressure metamorphic rocks and their tectonic environment in northeastern China: Journal of South East Asian Earth Sciences 3, 303-313.

Yarmolyuk, V.V., Kovalenko, V.I., Salnikova, E.B., Kozakov, I.K., Kotov A.B., Kovach, V.P., Vladykin, N.V., Yakovleva, S.Z., 2005. U–Pb age of syn- and post-metamorphic granitoids of south Mongolia:evidence for the presence of Grenvillides in the Central Asian Foldbelt. Doklady Earth Sciences 404:986–990.

Zhai, M.G., Li, T.S., Peng, P., Hu, B., Liu, F., Zhang, Y.B., 2010. Precambrian key tectonic events and evolution of the North China Craton. In: Kusky, T.M., Zhai, M.G., Xiao,W.J. (Eds.), The Evolving Continents: Understanding Processes of Continental Growth. Geological Society, London Special Publication, 338. pp. 235–262.

Zhang, H.T., So, C.S. Yun, S.T., 1999. Regional geologic setting and metallogenesis of central Inner Mongolia, China: guides for exploration of mesothermal gold deposits. Ore Geology Reviews 14, 129-146.

Zhang, C., Wu, T.R., 1999. Features and tectonic implications of the ophiolitic mélange in the southern Suzuoqi, Inner Mongolia. Scientia geologica sinica 34, 381-389. (in Chinese with English abstract).

Zhang, W., Jian, P., Kröner,A., Shi, Y.R. 2012. Magmatic and metamorphic development of an early to mid-Paleozoic continental margin arc in the southernmost Central Asian Orogenic Belt, Inner Mongolia, China. Journal of Asian Earth Sciences, DOI:http://dx.doi.org/10.1016/j.jseaes.2012.05.025

Zhao, G. C., Sun, M. Wilde, S., 2005. Late Archean to Paleoproterozoic evolution of the North China Craton: key issues revisited. Precambrian Research 136, 177-200.

Zhao, L., Wu, T.R., Luo, H.L., He, Y.K., Jing, X.,2008. Geochemistry of Huheengeer Complex, Bayan Obo Region, Inner Mongolia and its tectonic implications. Geological Journal of China Universities 14, 29-38. (In Chinese with English abstract).

Zhu, Y.F., Sun, S.H., Mao, Q., Zhao, G., 2004. Geochemistry of the Xilingele Complex, Inner Mongolia: a historic record from Rodinia accretion to continental collision after closure of the Paleo-Asian Ocean. Geological Journal of China Universities 10, 343-355. (In Chinese with English abstract).

Figure captions

Fig. 1 Tectonic sketch map of central Inner Mongolia modified from Badarch et al. (2002), Xiao et al. (2003) and Xu et al. (2012). The late Mesozoic-Cenozoic formations are omitted for clarity. SME = Southern Margin of Ergun block; NOB = Northern Orogenic Belt; HB = Hunshandake block; SOB = Southern Orogenic Belt; NCC = North China Craton. The double spot dash line representing the Solonker Suture and the names in brackets and italics are from Xiao et al. (2003).

Fig. 2 Geological map of the Hongqi area in Inner Mongolia showing litho-tectonic units distribution. Modified after IMBGMR (2002, 2008).

Fig. 3 Geological map (A), cross section (B), and structural elements of the Hongqi mélange (C-F; lower hemisphere projection). Modified after IMBGMR (2002, 2008).

Fig. 4 Field pictures in the Hongqi mélange unit. (A) Blocks of limestone and volcanite embeded in the matrix; (B) Early Devonian basal conglomerates cropping out close to the mélange ; (C) Foliated limestone containing elongated Silurian fossils included as block in the Hongqi mélange; (D) Undeformed Early Devonian basal conglomerates including rounded pebbles of volcanic rocks, greenschist, chert and quartzite.

Fig. 5 Field pictures in the Hongqi mélange unit. (A) Stretching lineation in chlorite quartz schist; (B) Intrafolial fold (F_1) with SE-NW striking axis; (C) Pinch-and-swell structure within quartz schists; (D) Flattened and elongated pillow lavas block in the

mélange; (E) asymmetrical fold (F_2) with SE-dipping long limb indicating northwest

vergence; (F) Asymmetric kink bands F_2 refolded L_1 stretching lineation; (G) Northeast

striking upright fold (F_3) developed in quartz chlorite schist; (H) Upright fold formed in

quartz-rich layer.

Fig. 6 Microscope scale kinematic indicators in the Hongqi mélange. A~G thin sections

are cut perpendicular to the main S_1 foliation, and parallel to the L_1 stretching lineation.

(A) Geometric relationship between bedding (S_0) and foliation (S_1) in the hinge of an

intrafolial fold in metapelite; (B) oriented alignment of amphibole and anhedral quartz

indicating top-to-the WNW shearing; Am = Amphiolite, Pl = Plagioclase, Qtz = Quartz,

Chl = Chlorite; (C), (D) asymmetrical chlorite fibers developed as pressure shadows

constitutes oriented chlorite fibers around the end of a feldspar clast, showing a

northwestward shearing; (E) oblique fractured carbonate grains showing a

top-to-northwest NW shearing; (F) Boudinage of feldspar clast with recrystallized

chlorite fibers in the interspace, suggesting SE-NW stretching direction; (G) Mica

bands defined by curved recrystallized mica aggregates and insoluble material,

showing northwest ward shearing; (H) Sigmoidal clast indicating top-to-N shearing.

Fig. 7 Sketch map (A), cross section (B), and structural elements of Ondor Sum area (C,

D; lower hemisphere projection). modified after IMBGMR (1976). The Cenozoic trap

basalts must not be confused with the basaltic blocks included in the mélange.

Fig. 8 Field pictures in the Ondor Sum area. (A) Typical field aspect of the Ondor Sum colored mélange due to various blocks of pillow basalts, chert, limestone, sandstone enclosed in a greenschist sandy-silty matrix; (B) Colored conglomerate with red chert, white limestone, green lava or volcanic-sedimentary material in the Ulan Valley; (C)(D) Amphibolite and gneissic granite dykes in the Tulinkai and Ulan Obo areas; C: amphibolite-acidic gneiss metre-sized alternation; D: folded amphibolite cross cut by a granitic dyke; (E) Vertical foliation (S_1) and mineral lineation (L_1) in green chlorite-epidote schist in the southern part of the Ondor Sum mélange unit. (F) Mineral and stretching lineation (L_1) folded around an F_2 fold, Ulan valley; (G) L_1 stretching lineation deformed by an SE-verging F_2 fold axis (L_2:F_2 fold axis), Ulan valley; (H) Microfold associated with a crenulation cleavage (S_2) in Ulan valley

Fig. 9 Structural map of the microtectonic data observed in the Ulan valley (modified after Xiao et al., 2003).

Fig. 10 Microscope scale kinematic indicators in the Ondor Sum mélange. All cross sections are cut perpendicular to the main S_1 foliation, and parallel to the L_1 stretching lineation. (A) (B) (C) Sigmoidal feldspar and carbonate porphyroclast showing top-to-the-NW shearing, southern limb of Ondor Sum mélange; (D) Sigmoidal feldspar porphyroclast showing a top-to-the-NW sense of shear in the middle part of the Ondor Sum mélange; (E) subvertical S_3 cleavage cutting the S_1 foliation; (F) Crenulation cleavage oblique to the main foliation S_1. Syn-S_1 chlorite is deformed by D_2 folding;

(G) Asymmetric pressure shadow around quartz aggregates showing a top-to-the NW sense of shear, Ulan valley; (H) Carbonate sigmoidal porphyroclast showing a top-to-the-NW sense of shear, Ulan valley;

Fig. 11 (A) Representative CL image of dated zircons. (B) U-Pb Concordia diagrams for sample 090716-29 of acidic volcanite (The data ellipses are defined by standard errors (1 sigma) in $^{206}Pb/^{238}U$, $^{207}Pb/^{235}U$ and $^{207}Pb/^{206}Pb$. Grey ellipses represent inherited zircons. The data with age concordance >10% are not projected in the concordia diagram.

Fig. 12 Interpretative crustal scale cross section of the Southern Orogen of Inner Mongolia, showing the Early Paleozoic accretion-collision belt. The position of this cross section is shown in Figs. 1 and 2.

Fig. 13 Tentative Paleozoic geodynamic evolution model of the southern belt of Inner Mongolia (see text for detail).

Table 1 Summary of geochronological data for the Hongqi-Ondor Sum area. The number in the parentheses corresponds to those in Fig. 2, Fig. 7 and Fig. 9 respectively.
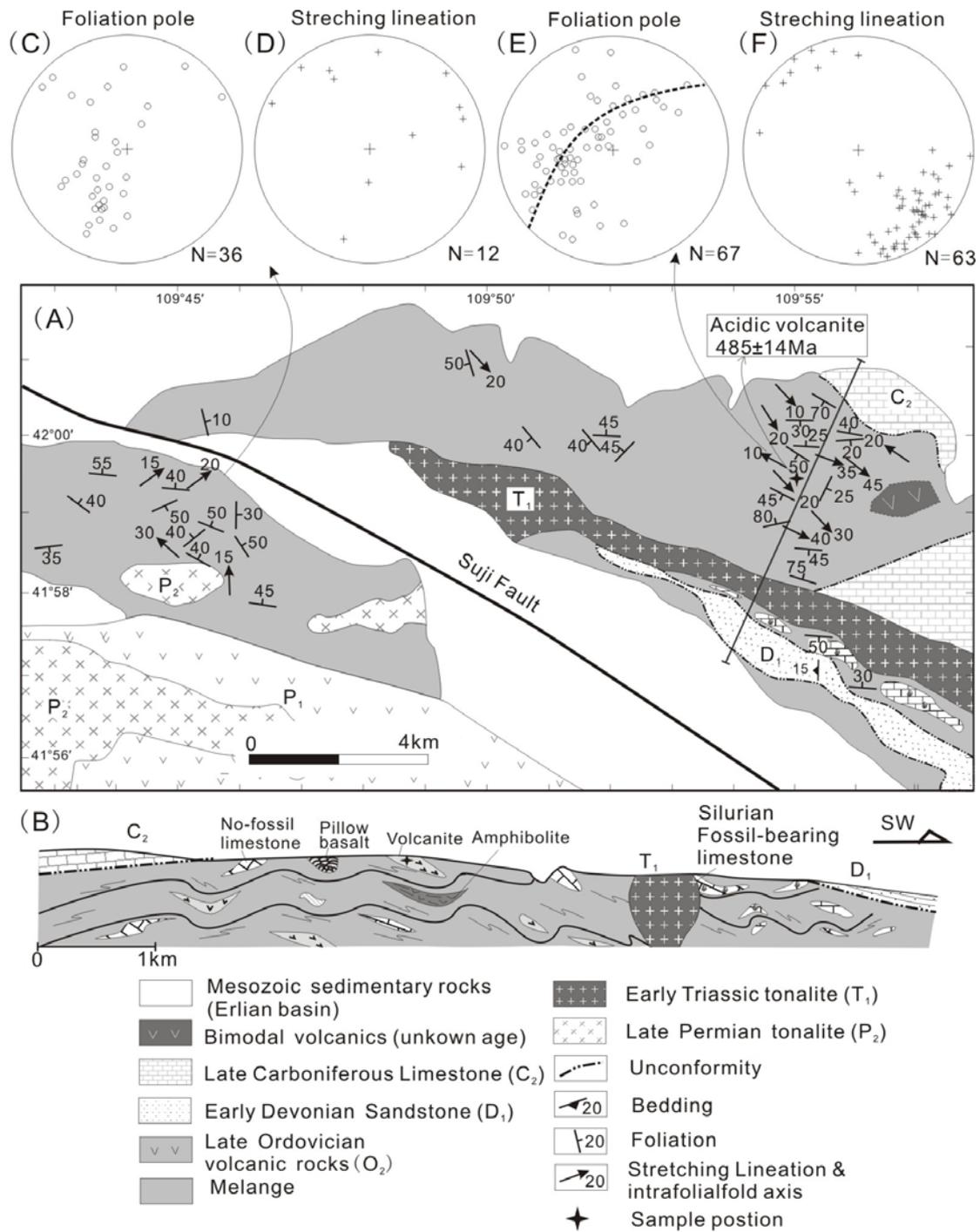
Table 2 ICP-MS U-Pb data for the magmatic zircons.
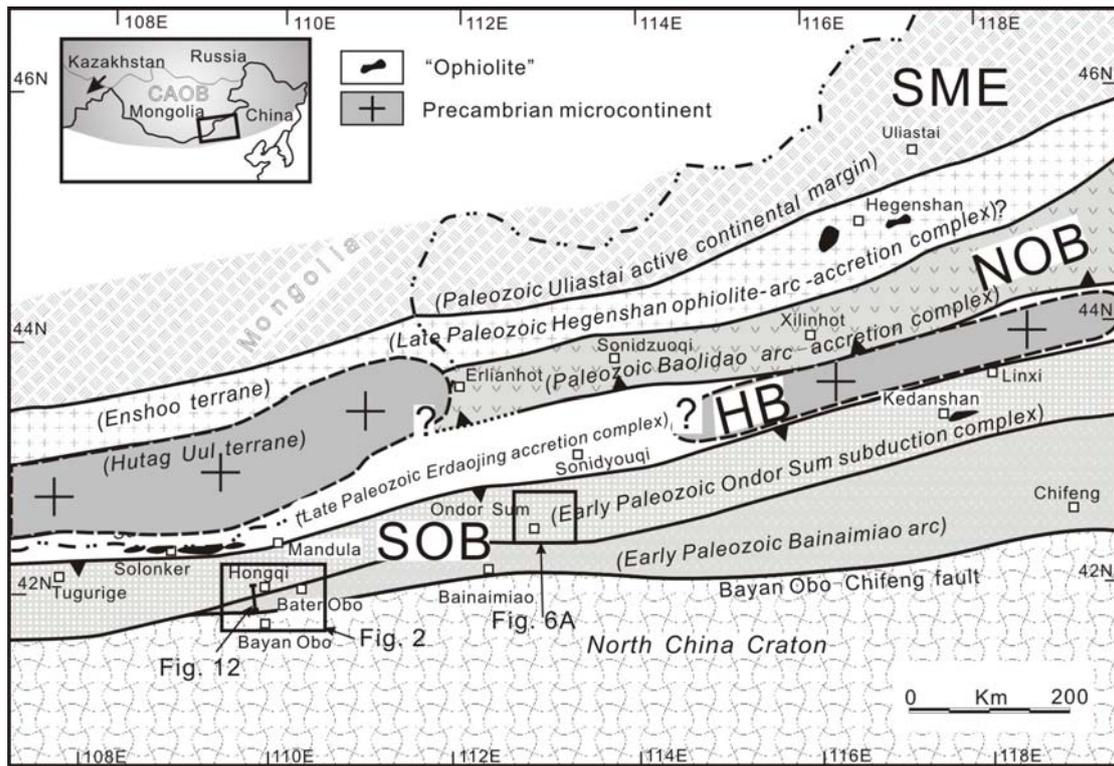
Figure 1
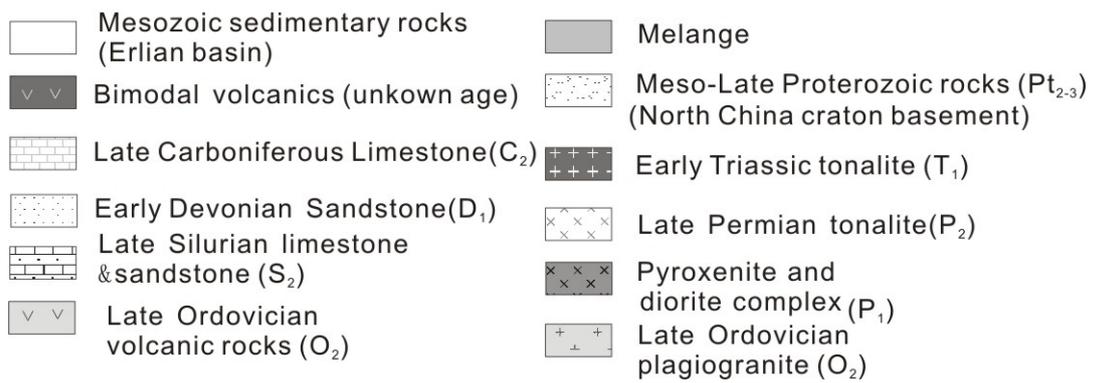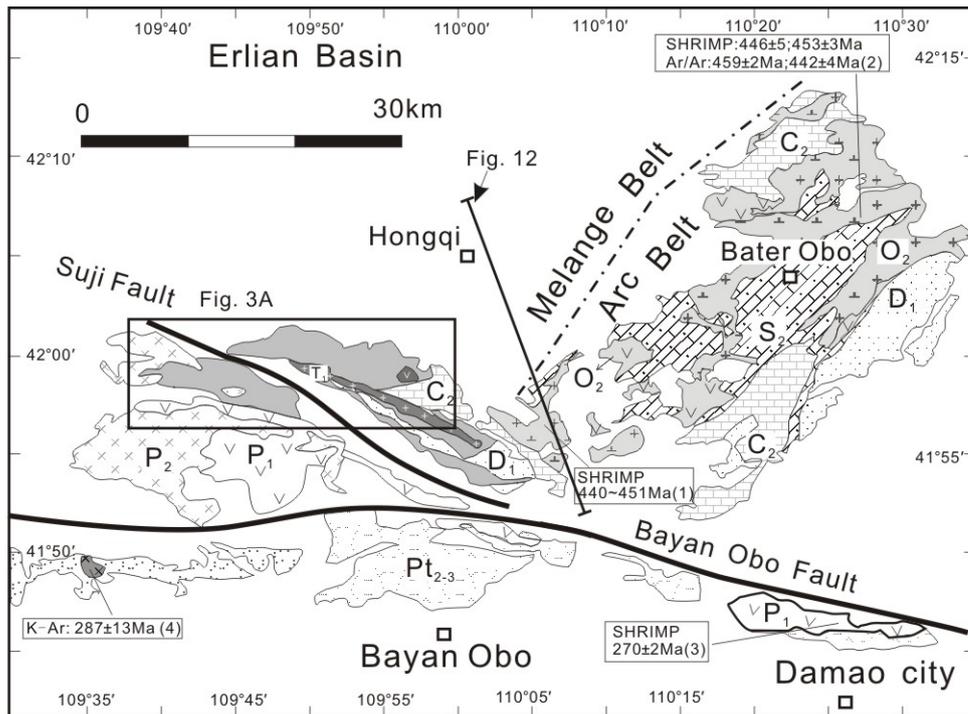
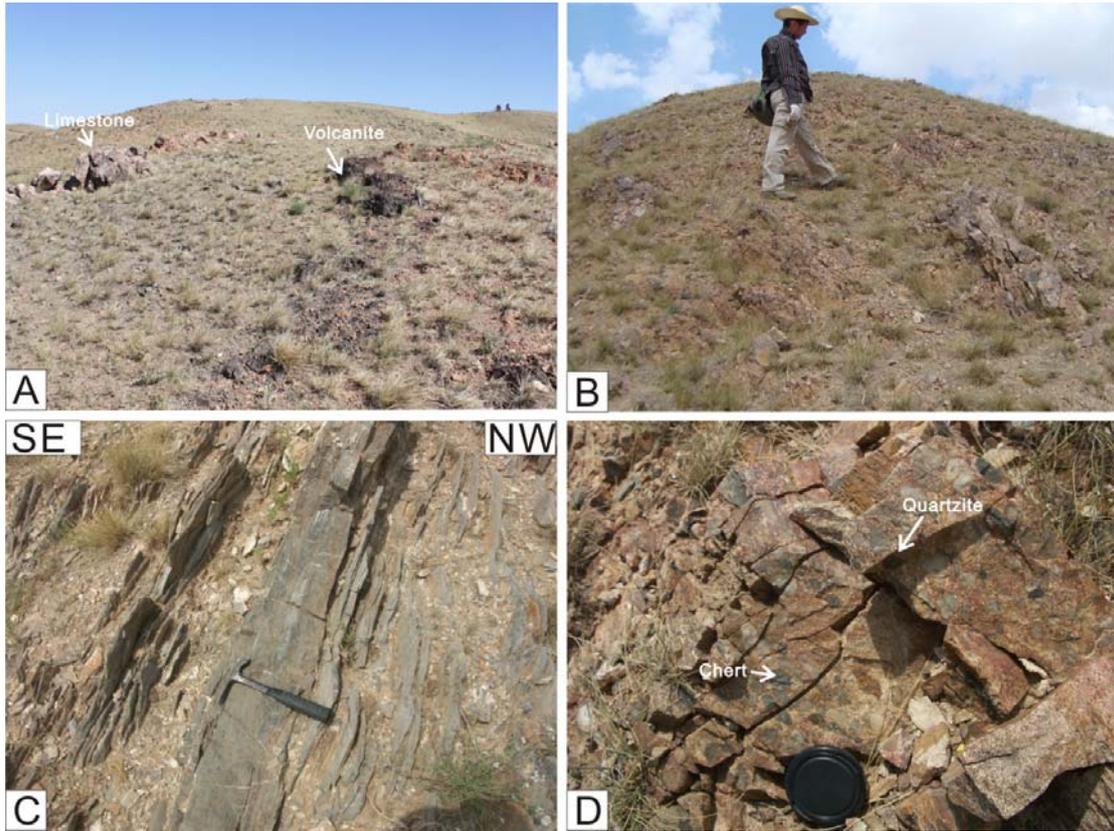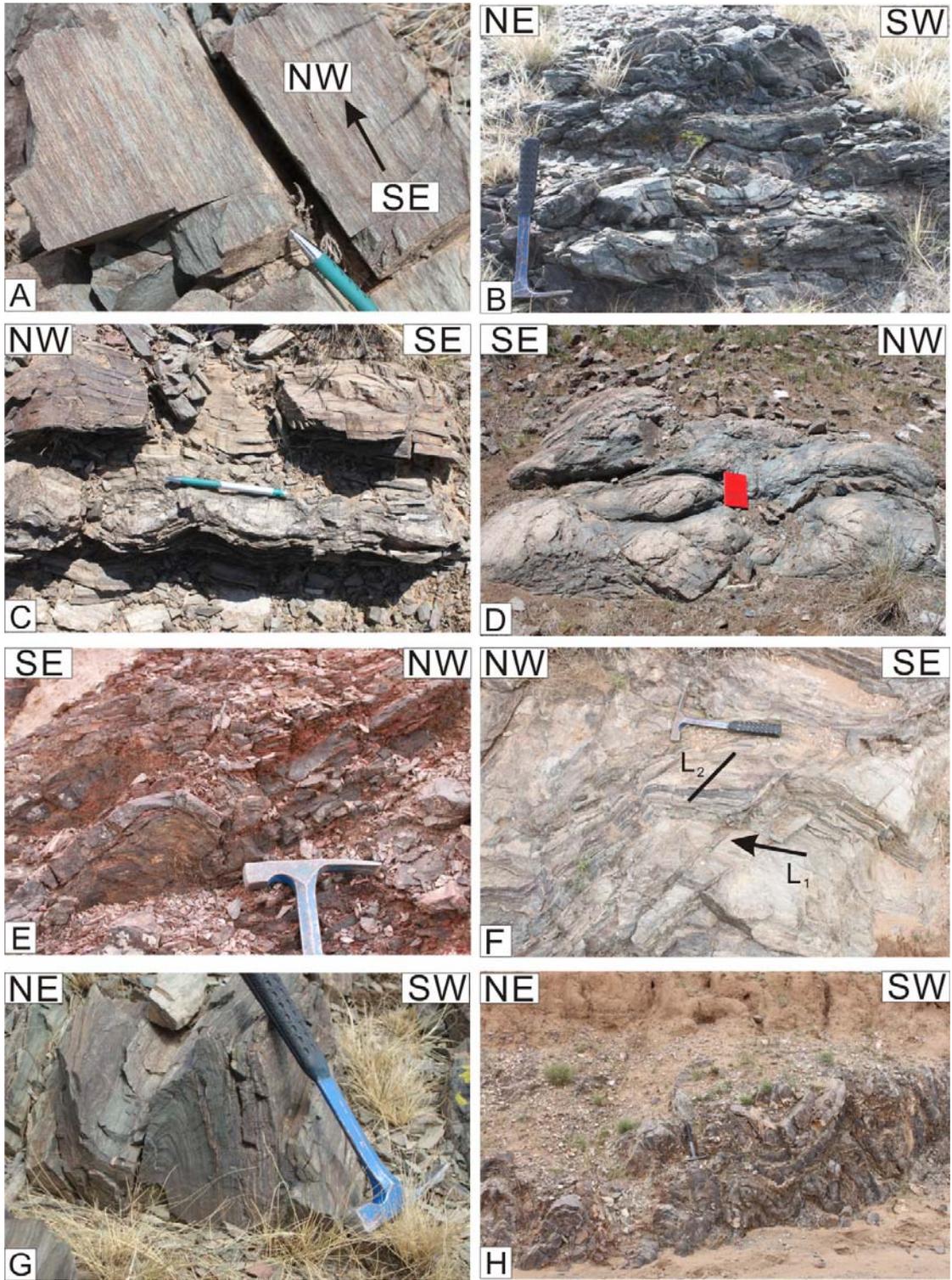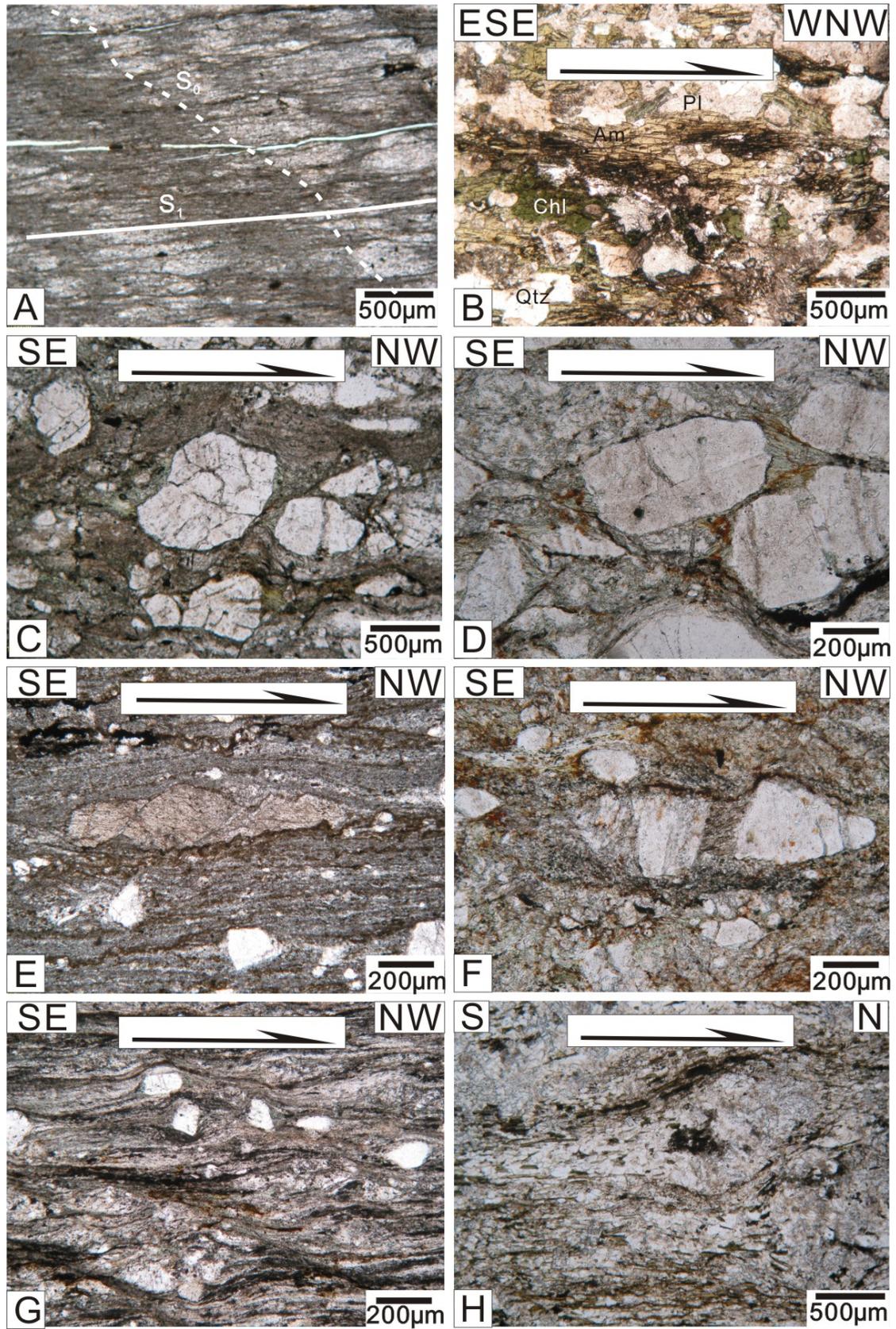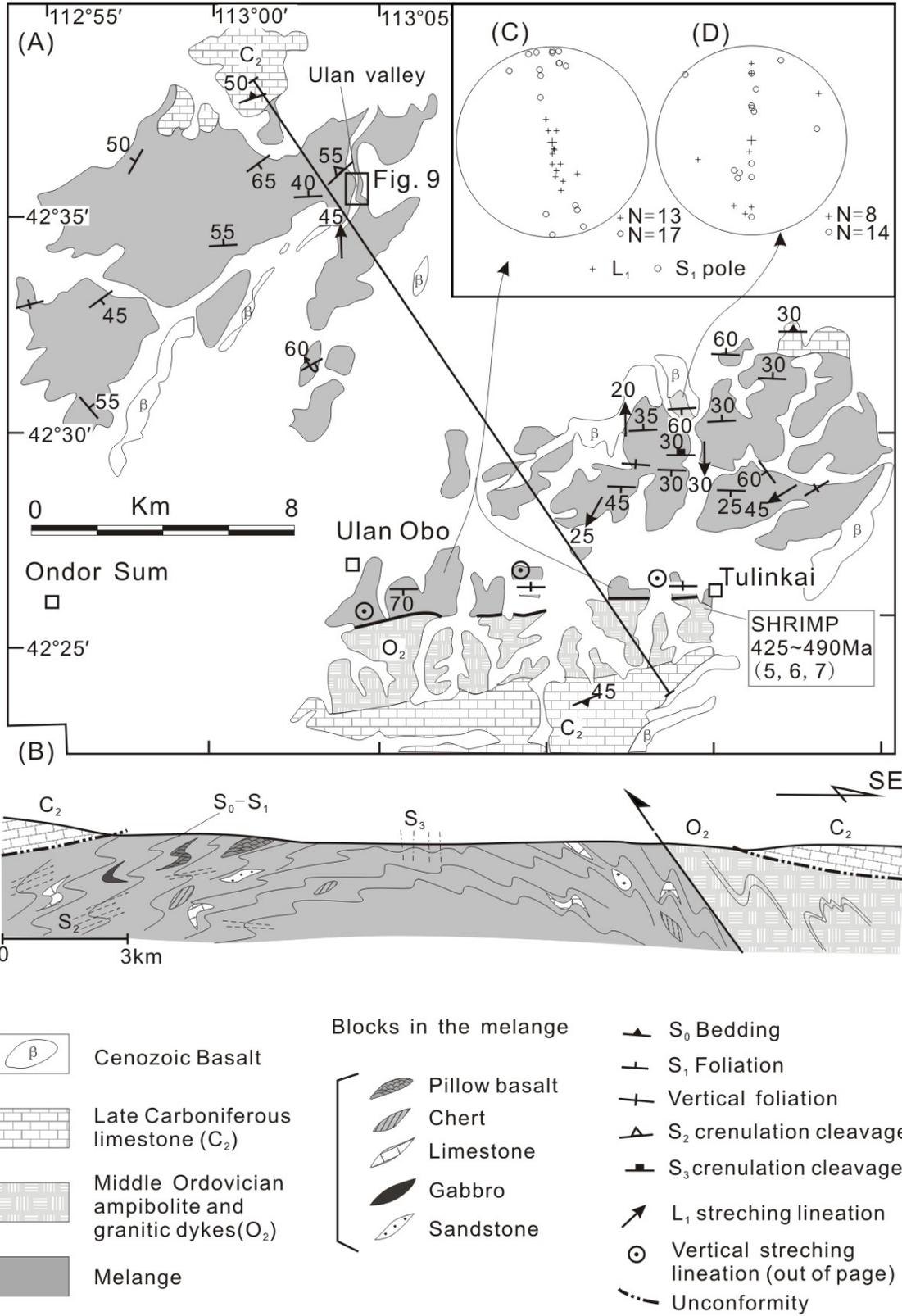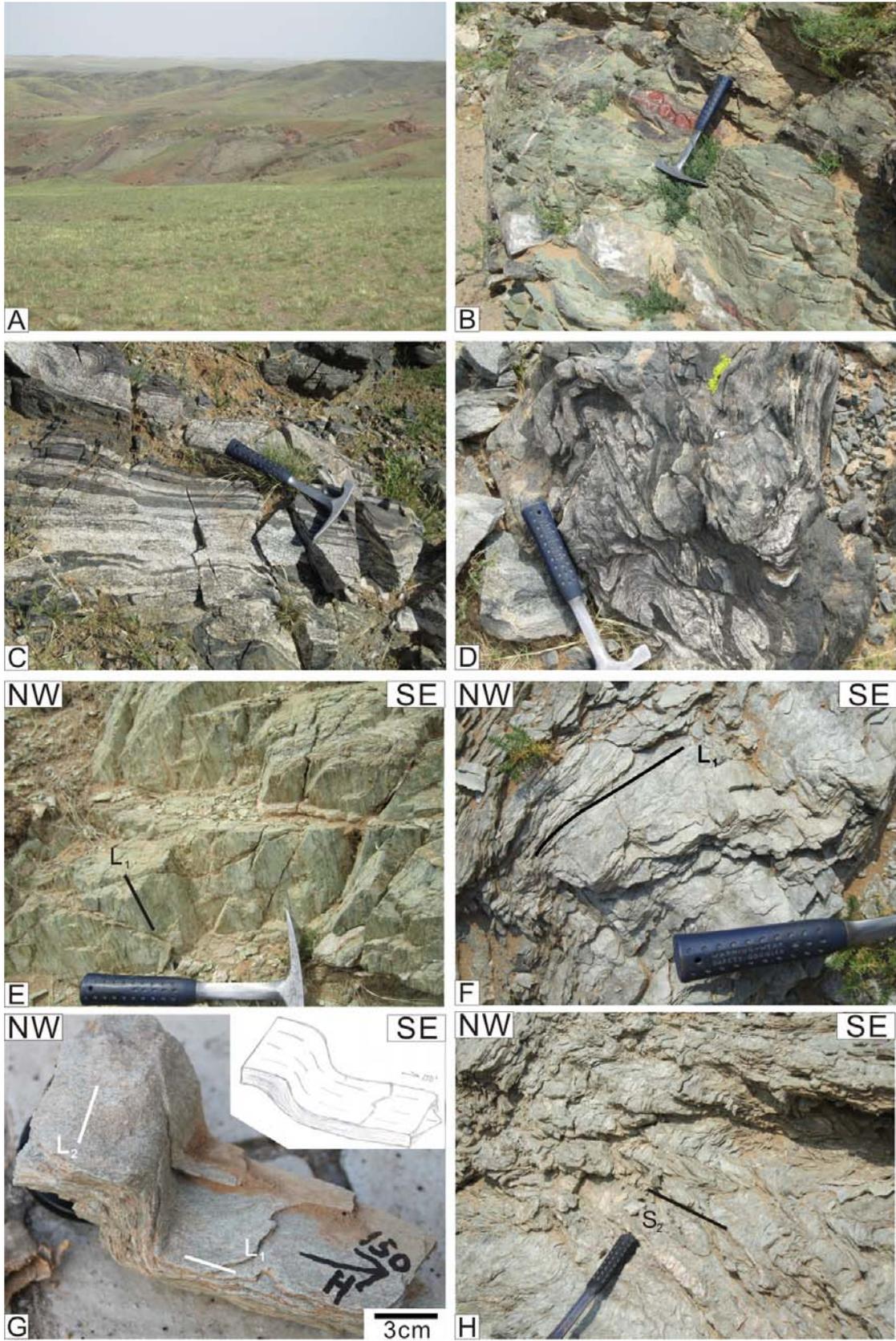Figure 2

Figure 3

Figure 4

Figure 5

Figure 6

(A)

112°55' 113°00' 113°05'

C₂

Ulan valley

50

50

65 40

55

45

Fig. 9

—42°35'

55

45

60

—42°30'

55

β

β

0   Km   8

Ondor Sum

Ulan Obo

70

—42°25'

O₂

C₂

(B)

(C)   (D)

N=13
N=17

N=8
N=14

+ L₁   ○ S₁ pole

30

60

30

30

20

35 60

30

30 30

45

25

45

60

25 45

β

Tulinkai

SHRIMP
425~490Ma
(5, 6, 7)

(B)

C₂   S₀–S₁   S₃   O₂   C₂   SE

S₂

0   3km

Figure 7

	Cenozoic Basalt
	Late Carboniferous limestone (C₂)
	Middle Ordovician ampibolite and granitic dykes(O₂)
	Melange

Blocks in the melange

Pillow basalt

Chert

Limestone

Gabbro

Sandstone

S₀ Bedding

S₁ Foliation

Vertical foliation

S₂ crenulation cleavage

S₃ crenulation cleavage
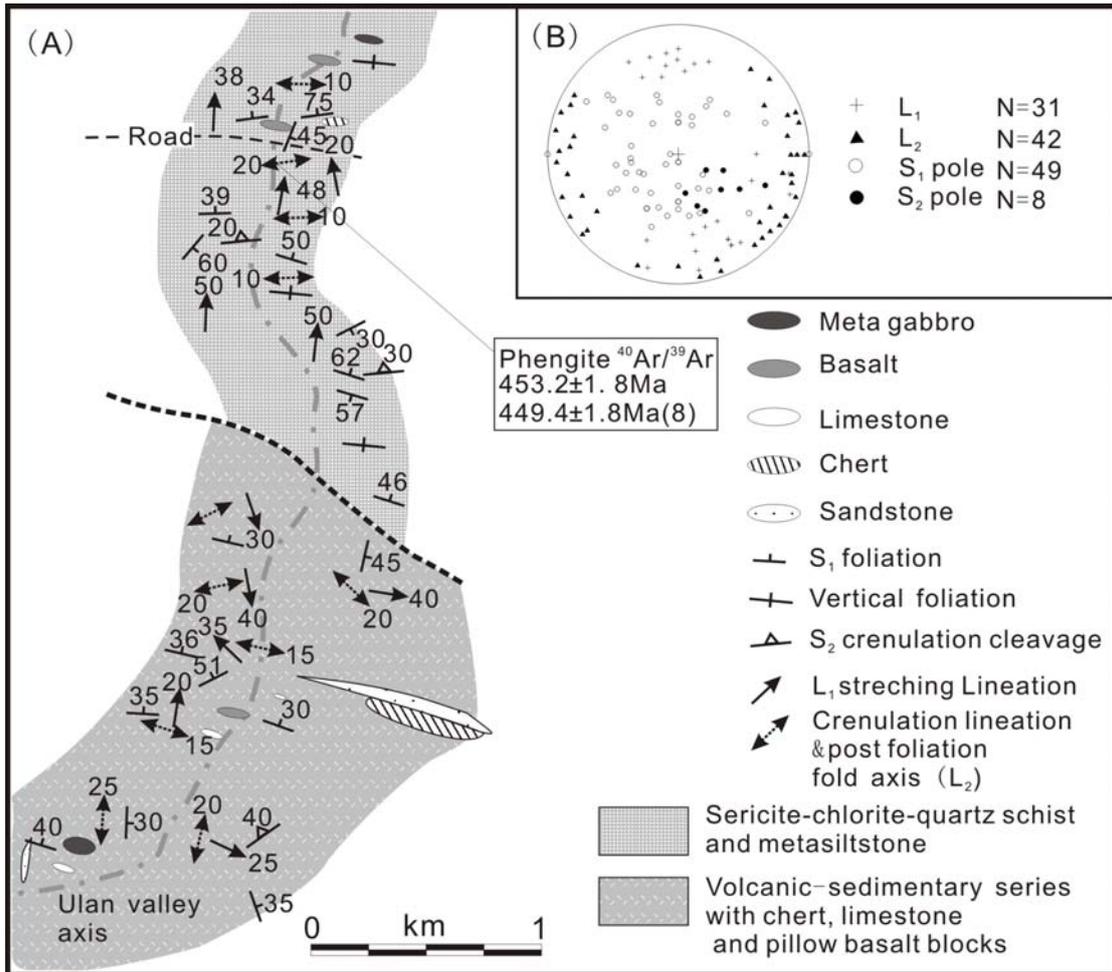
L₁ streching lineation

Vertical streching lineation (out of page)
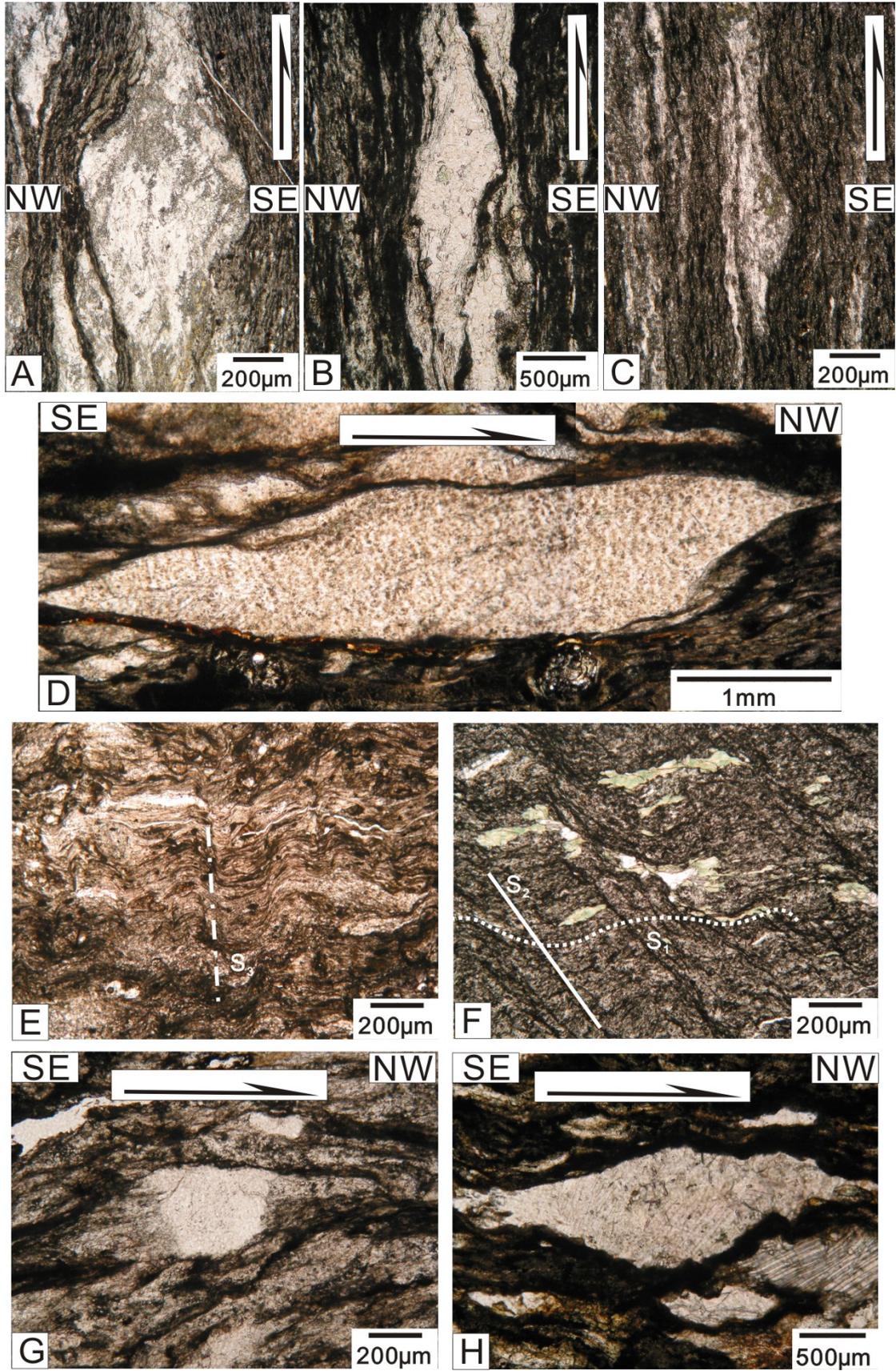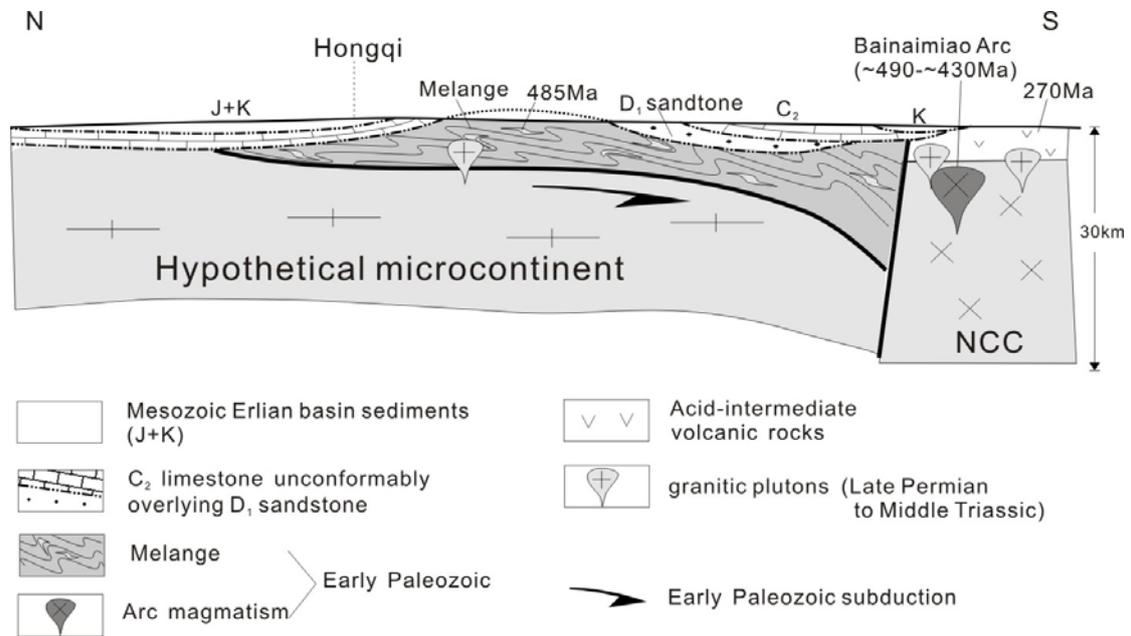
Unconformity

Figure 8

Figure 9

Figure 10
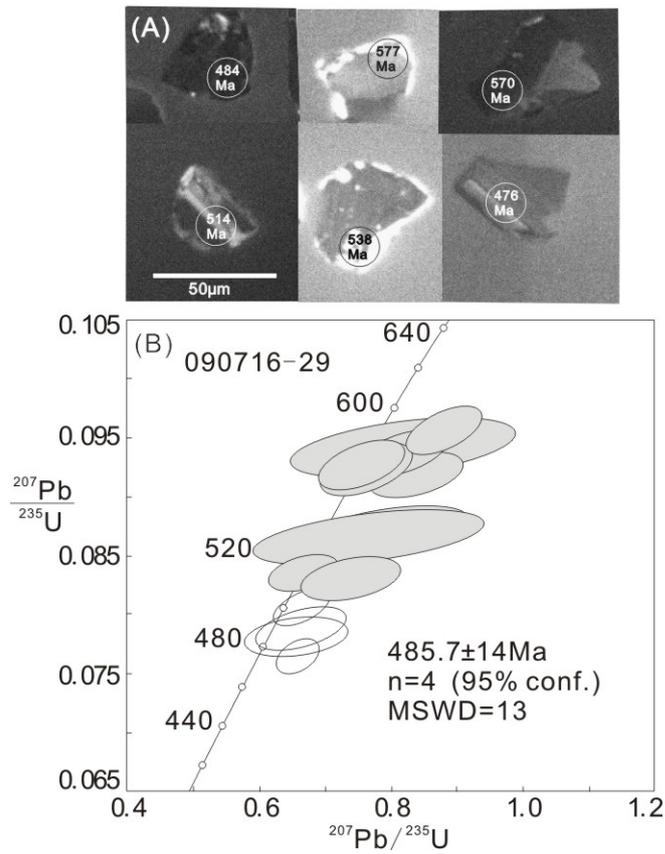
Figure 11

Figure 12

(A) ~550-~420Ma   Early Paleozoic: subduction accretionary orogen

N

Hypothetical
microcontinent

Hongqi-Ondor Sum
accretionary complex

Bainaimiao arc

North China Craton

S
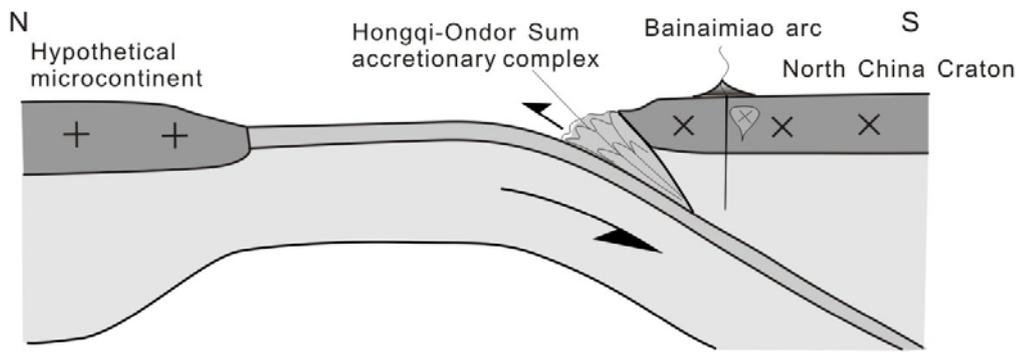
(B) ~420-~300Ma   Early Devonian-Late Carboniferous: post-collisional deposits

N

Platform limestone (C₂)
D₁ sandstone

S

Suture zone

Figure 13